Sub-THz Ray Tracing Simulation and Experimental Validation for Indoor Scenarios

Yuan, Zhiqiang; Lyu, Yejian; Zhang,, Jianhua; Tang, Pan; Liu, Ximan; Lin, Jiaxin; Petersen, Sigurd Sándor; Fan, Wei

Published in:
2023 IEEE International Mediterranean Conference on Communications and Networking, MeditCom 2023

DOI (link to publication from Publisher):
10.1109/MeditCom58224.2023.10266598

Publication date:
2023

Document Version
Accepted author manuscript, peer reviewed version

Sub-THz Ray Tracing Simulation and Experimental Validation for Indoor Scenarios

Zhiqiang Yuan[12], Yejian Lyu[2], Jianhua Zhang[1], Pan Tang[1], Ximan Liu[1],
Jiaxin Lin[1], Sigurd S. Petersen[2], and Wei Fan[3*]
[1] Beijing University of Posts and Telecommunications, Beijing, China
[2] Antenna, Propagation, and Millimeter-wave Systems Section, Aalborg University, 9220 Aalborg, Denmark
[3] National Mobile Communications Research Laboratory, School of Information Science and Engineering, Southeast University, Nanjing 210096, China

***Abstract*—Sub-terahertz (THz) communication is envisioned as one of the key components for 6G because of the abundantly available spectrum resource. Accurate and efficient channel models are prerequisites for developing sub-THz communication systems. Due to the sparsity and more ray optics propagation characteristics of the sub-THz channel, deterministic Ray-Tracing (RT) has attracted much attention for sub-THz channel modeling, which shows the potential of reducing the simulation complexity yet maintaining the accuracy. This paper presents an implementation of RT for sub-THz channel modeling and demonstrates its performance based on sub-THz channel measurements. A virtual massive multiple-input-multiple-output (MIMO) channel operating at 100 GHz and a double-directional 300 GHz channel are considered in the RT implementation, where the RT achieves a high similarity compared to the channel measurements in terms of channel impulse response and power angular spectrum. Besides, the near-field and spatial non-stationary properties of the sub-THz massive MIMO channel and the dominant multipaths of the 300 GHz channel are accurately reconstructed in the RT simulation. This work can provide insights into deterministic sub-THz channel modeling research from the implementation, evaluation, and challenges perspectives.**

***Index Terms*—Sub-terahertz, Ray-Tracing, channel measurement, channel modeling.**

I. Introduction

In pursuit of more bandwidth and high data rate transmission in applications nowadays, researchers have started to exploit the sub-terahertz (sub-THz) band for wireless communications. Sub-THz communication offers abundant spectrum resources, making it highly attractive for various application scenarios, such as sixth-generation (6G) short-range cellular communication, and sensing applications [1]–[6]. However, the sub-THz channel exhibits different channel properties compared to lower frequency bands, e.g., sub-6 GHz bands. The sub-THz channel experiences significant propagation loss due to high free-space path loss and noticeable atmospheric molecular absorption [7]–[9]. To compensate for this loss and accommodate the power limitations of current sub-THz transceivers, high-gain directional antennas should be employed at the transmitting (Tx) or receiving (Rx), or both sides.

The channel models can be categorized into two types i.e.: statistical and deterministic. The statistical models rely on channel measurements to obtain adequate channel data. Directional scanning schemes (DSSs) [10]–[14] or virtual large-scale antenna arrays [15] are used in the channel measurement at such high-frequency bands, which makes the channel measurements more time-consuming. So far, no standard statistical channel models have been developed. As for deterministic models, Ray-Tracing (RT) is a promising simulation approach [16]–[18]. Only a handful of RT validations were reported in the literature. Sub-THz channel measurements and RT simulation were conducted in the indoor office and meeting room scenarios in [19], [20]. Both of the RT results show a good agreement with the measurement results. Besides, in [21]–[23], channel measurements were conducted in vehicular scenarios, e.g., intrawagon and vehicle-to-infrastructure scenarios, the measurement results were utilized to validate RT and then the RT simulation was extended to various combinations of transmitter deployments and scenario conditions. With the lack of material properties and understanding of propagation mechanisms in sub-THz bands, the accuracy of the RT is limited [24]. Besides, with the wavelength of the sub-THz bands approaching the millimeter level, the digital map of the scenario is required to be more precise for accurate RT simulation, which increases the computation complexity. However, the sub-THz channel shows to be sparse and specular, only with a few dominant propagation paths, and the paths are susceptible to blockage in state-of-the-art works [21], [25], [26]. With these phenomena, the site-specific RT method can be utilized, which reduces the simulation complexity while maintaining accuracy.

In this paper, an RT-based deterministic method is presented for sub-THz bands. Besides, channel measurements in two different indoor scenarios, i.e., a clean room and a big hall, are conducted to calibrate and validate the RT simulation results. Good agreements are observed in the comparison between the measurement results and the RT results, which demonstrates the effectiveness of RT at sub-THz bands.

The rest of the paper is organized as follows: Section II describes the measurement scenarios, channel sounder, measurement configurations, and RT settings. The measurement results and RT simulation results are presented and analyzed in Section III. Section IV draws the conclusions.

II. Measurement Campaigns and RT Simulations

We conducted sub-THz channel measurements and corresponding RT simulations for experimental validation. Two typical indoor scenarios, i.e., an empty room and a big hall, were considered. In the room scenario, a massive multiple-input-multiple-output (MIMO) channel at 100 GHz was measured with the virtual antenna array (VAA) scheme and then was simulated by the RT. In the big hall scenario, a sub-THz channel at 300 GHz was measured with double DSS (DDSS) and then was simulated by the RT. Finally, results from the measurements and simulations will be compared to evaluate the performance of RT simulations. This section will introduce the measurement campaigns and RT simulations in the following.

A. Measurement Campaigns

The measurements were conducted at Aalborg University, Denmark. Fig. 1 illustrates the room scenario, where a sub-THz massive MIMO channel measurement at 100 GHz and a corresponding RT simulation are presented. The room is in the dimension of $8.19 \times 4.78 \times 3.1$ m^3. A virtual antenna array (VAA) was formed as the Rx by using a rotator, where a uniform circular array (UCA) with a diameter of 1 m and 2400 elements was realized. A single antenna was employed as the Tx. The VAA measurements require a coherent phase performance over all the array elements. Thus, a phase-compensated vector network analyzer (VNA)-based channel sounder (in the top of Fig. 3), which has a stable system phase and can support phase-coherent measurements, was used in these measurements. Readers can refer to [15] for the detailed principle and performance of the channel sounder. The VNA is set to sweep from 95 to 105 GHz with 6001 frequency points and 500 Hz IF bandwidth, which results in a delay resolution of 0.1 ns and a maximum detectable distance of 180 m. Identical omnidirectional antennas with 4.5 dBi antenna gain were applied to both the Tx and Rx. The distance between the Rx UCA center and the Tx was 6.5 m, and the antenna height was 1.25 m. A metallic board with a length of 0.57 m was placed between the Rx array and Tx, which would lead to the blockage of the line-of-sight (LoS) path for partial array elements. This setting aims to significantly observe the spatial-non-stationary (SnS) phenomenon in the sub-THz massive MIMO channel. Fig. 1 (bottom) illustrates the RT simulation for the scenario, whose details are described later. As shown, a room with the same dimensions as the real world was built in the RT simulator. Objects in the room, including doors, an elevator, radiators, floor, and ceiling were reconstructed as well.

The big hall scenario is in dimensions of $60 \times 20 \times 10$ m^3. As shown in Fig. 2, a DDSS-based sub-THz channel measurement at 300 GHz and a corresponding RT simulation were conducted. In the measurement, a radio-over-fiber (RoF)-enabled VNA-based sounder [25] (in the bottom of Fig. 3) was utilized to measure the channel. The frequency sweeping range is 299-301 GHz in the VNA with 1001 frequency points and 2 kHz IF bandwidth. Two rotators were used to realize the DDSS of the channel, where two standard gain horn antennas with 26 dBi antenna gain mounted at the rotator centers were rotated to spatially scan the electromagnetic environment. The Tx is set to rotate from -90° to 90° with 4° rotation step, while the Rx rotates from -180° to 180° with 4° rotation step. Note that the scanning direction is specified in Fig. 2 (bottom). The distance between the Tx and Rx was 4.2 m. Fig. 2 (bottom) illustrates the RT simulation in the big hall scenario. As shown, the scenario with the same dimensions and objects as the real world was built in the RT simulator.

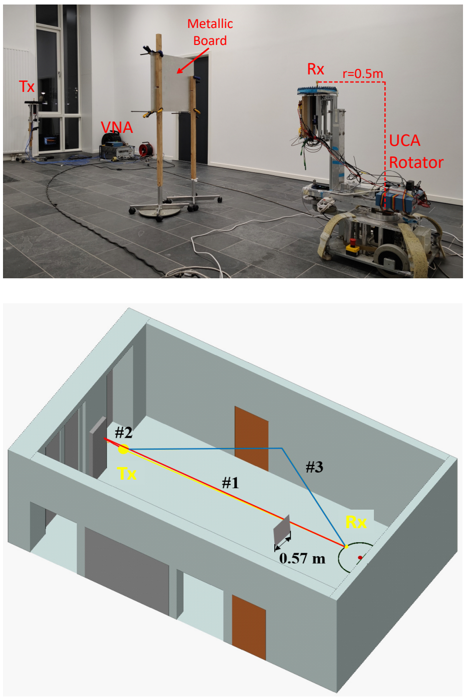

Fig. 1. The room scenario. A photo during the measurement (top) and illustration of RT simulation (bottom).

TABLE I
Measurement Setup

Scenarios	Indoor room	Big hall
Frequency (GHz)	95-105	299-301
Antenna type	Omni	Horn
Antenna gain (dBi)	4.5	26
Antenna HPBW (deg)	–	8
Tx rotation range (deg)	–	[-90:90]
Tx rotation resolution (deg)	–	4
Rx rotation range (deg)	[-180:180] (VAA)	[-180:180] (DSS)
Rx rotation resolution (deg)	0.15	4

B. RT Simulations

In this paper, a commercial RT simulator, Wireless InSite [27], was used for the RT simulations. The simulator has been widely used and experimentally validated in millimeter-wave frequency bands. In the simulations, the ray tracer was set to be limited to 4 reflections, 1 diffraction, and 1 penetration after considering the simulation complexity and accuracy. Note that we only focus on several multipaths

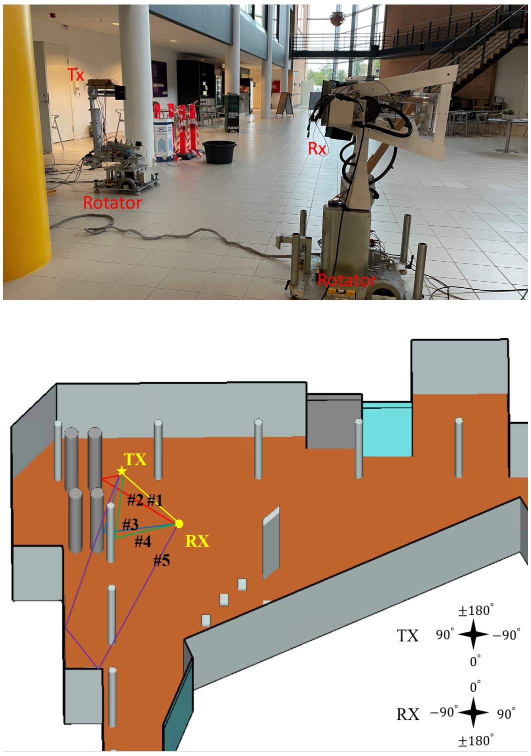

Fig. 2. The big hall scenario. A photo during the measurement (top) and illustration of RT simulation (bottom).

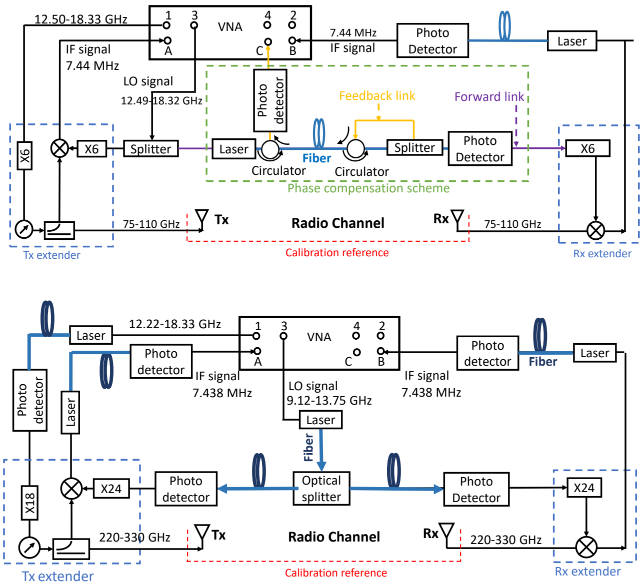

Fig. 3. Channel sounders built for the measurements, including the one operating at 100 GHz in the room scenario (top) and the one operating at 300 GHz in the big hall scenario (bottom).

with the strongest power in the simulations, since sub-THz communication will mainly rely on those dominant paths for data transmission as discussed.

As mentioned before, the real-world scenarios were precisely reconstructed in the simulator. In the room scenario, the same configurations as the measurement, e.g., the adopted omnidirectional antennas, operated frequencies, and bandwidth, were used for the simulation. The material parameters of objects were set according to the International Telecommunication Union (ITU) recommendations P.2040 [28], which provides material information for 0.001-100 GHz. Regarding the Rx array, 2400 elements were separately constructed in the simulator and a brute-force RT simulation was performed. Note that this method can realistically capture the near-field (NF) and SnS properties of massive MIMO channels [29], yet its process uses a lot of computational power and it is time-consuming. In total, the simulation took around 10 hours to complete the calculations for all VAA elements.

The same big hall scenario was reconstructed in the RT simulation, as shown in Fig. 2 (bottom). Most simulation configurations were the same as the measurement, including the frequency, Tx-Rx positions, height, etc. However, instead of directional antennas used for DSS measurements, two isotropic antennas were adopted as the Tx and Rx, respectively, to directly detect the spatial channel in the simulation. The simulated frequency was set to 300 GHz. Since the existing material documents, such as ITU-R P.2040, have not accurately covered 300 GHz, a calibration process on material parameters based on the measurement results was performed for the simulation. The material parameters were first set as that for 100 GHz according to ITU P.2040 and then were tuned by comparing the simulated paths and measured paths that interacted with objects. After the calibration process, a complete RT simulation at 300 GHz in the big hall scenario was performed.

III. Results and Analysis

This section presents and compares results obtained from the measurements and RT simulations in the two scenarios.

A. *Indoor Room Scenario*

Fig. 4 shows the channel impulse responses (CIRs) across antenna array elements in the indoor room scenario. The CIRs were obtained by performing an Inverse Discrete Fourier Transform (IDFT) on channel frequency responses (CFRs) that were collected by the VNA for each element. As shown from the measurement result i.e., Fig. 4 (top), the noise floor is around 105 dB. Multipaths are detected with an 's'-like curve in the element axis. It is due to the NF effect introduced by the large-scale array and ultra-wide bandwidth, where a path impinges with significantly different delays across array elements. Besides, several paths, are observed with the partial curve in the element axis, which means the paths have different responses to elements in different spatial locations. It is a result of the SnS property of the massive MIMO channel. For instance, it can be observed that the LoS path has an incomplete trajectory in the array axis, as a metallic board was set to block the LoS path for some

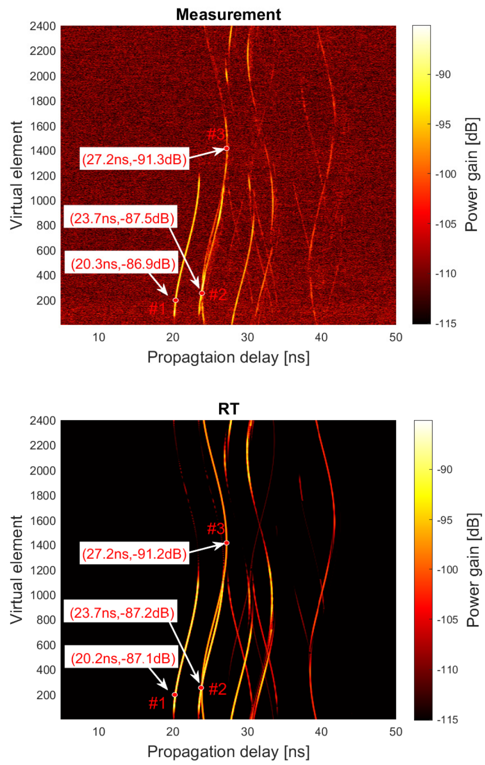

Fig. 4. CIRs across elements in the room scenario, obtained from (top) the measurement and (bottom) the RT simulation.

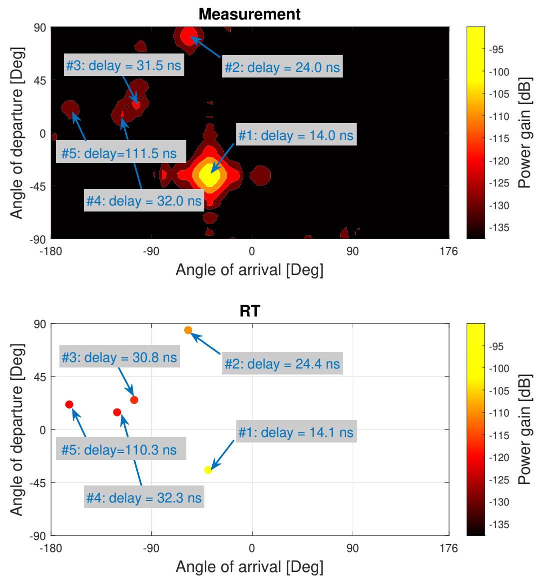

Fig. 5. PAS of the sub-THz channel in the big hall scenario, obtained from (top) the measurement and (bottom) the RT simulation.

elements as mentioned before. To capture those properties and experimentally validate the RT simulation, three paths are specifically marked in the figure. The path parameters are presented with one element as the reference.

A high similarity between simulated CIRs and measured CIRs is observed in Fig. 4. In the simulation results, i.e., Fig. 4 (bottom), multipaths are generated with the same 's'-like curve as that in the measurement. Besides, the SnS multipaths that have partial trajectories in the array axis are well reconstructed in the simulation. Those results demonstrate that the RT is able to capture the NF and SnS properties in the massive MIMO sub-THz channel. Moreover, corresponding to the measurement result, three multipaths are also marked with the parameters. It can be found that the RT can accurately simulate those multipaths in the sub-THz channel, where the path parameters are reconstructed with errors up to 0.1 ns and 0.3 dB in delay and power, respectively. Moreover, propagation trajectories of those paths are presented in Fig. 1 (bottom), which shows the paths' interactions with the environment and also further explains the SnS phenomena of the paths. Those results validate the RT ability for sub-THz massive MIMO channel modeling.

B. Big Hall Scenario

Fig. 5 illustrates the power angular spectrum (PAS) of the 300 GHz sub-THz channel in the big hall scenario, which shows the power distribution of the channel with angles of arrival and departure. Note that the PAS in the measurement result was obtained by adding up the power of measured CIR at all delay bins. In the measurement result, i.e., Fig. 5 (top), it can be observed that the power of the channel is mainly distributed on a few angles. Correspondingly, 5 dominant multipaths were estimated from the measured CIRs at those angles. The estimated paths are then marked in the figure.

Fig. 5 (bottom) shows the RT simulation result for the sub-THz channel. Note that we only focus on several dominant multipaths in this RT simulation as mentioned before. As shown, 5 paths are simulated in the simulation result, which matches with the measurement result well. Specifically, errors between the measured paths and simulated paths are within 1.8°, 0.7 ns, and 0.7 dB in terms of the angle, delay, and power, respectively. Those results show the ability of RT for the 300 GHz sub-THz channel modeling.

IV. Conclusion

This paper aims to experimentally validate the RT simulation for sub-THz channel modeling with measurements in two scenarios. In the indoor room scenario, a massive MIMO sub-THz channel at 100 GHz with 1 m length of array aperture and 2400 elements was measured with the VAA scheme and then simulated by the RT. A good similarity between the measured CIRs and simulated CIRs is realized, and the channel NF and SnS properties observed in the measurement are realistically captured by the RT simulation. In the big hall scenario, a double-directional sub-THz channel at 300 GHz was measured via the DDSS scheme with two rotators. Then, an RT simulation was conducted with the same scenario reconstructed. To obtain the material parameters at 300 GHz for the simulation, a calibration process on the materials based on the measurement result was performed. Several dominant multipaths were detected in the PAS in the channel measurement, and the RT accurately reconstruct those multipaths. Specifically, the errors between the measured paths and simulated ones are within $1.8°$, 0.7 ns, and 0.7 dB in terms of the angle, delay, and power, respectively. Those results validate the ability of RT for the sub-THz channel modeling. Nevertheless, some difficulties in RT simulations for sub-THz channel modeling, such as high simulation complexity for massive MIMO and the lack of material information at high frequencies, are also discussed preliminarily. This paper provides insights into deterministic sub-THz channel modeling research.

ACKNOWLEDGEMENT

The work was partially supported by the 21NRM03 MEWS project, which has received funding from the European Partnership on Metrology, co-financed from the European Union's Horizon Europe Research and Innovation Programme and by the Participating States. The work of BUPT was supported in part by the National Science Fund for Distinguished Young Scholars under Grant 61925102, in part by the National Natural Science Foundation of China under Grant 92167202, and in part by the BUPT Excellent Ph.D. Students Foundation under Grant CX2022202.

REFERENCES

[1] J. Zhang, J. Lin, P. Tang, W. Fan, Z. Yuan, X. Liu, H. Xu, Y. Lyu, L. Tian, and P. Zhang, "Deterministic ray tracing: A promising approach to THz channel modeling in 6G deployment scenarios," *IEEE Communications Magazine*, 2023.

[2] C. Chaccour, M. N. Soorki, W. Saad, M. Bennis, P. Popovski, and M. Debbah, "Seven defining features of terahertz (thz) wireless systems: A fellowship of communication and sensing," *IEEE Communications Surveys Tutorials*, vol. 24, no. 2, pp. 967–993, 2022.

[3] A. Pärssinen, M.-S. Alouini, M. Berg, T. Kürner, P. Kyösti, M. E. Leinonen, M. Matinmikko-Blue, E. McCune, U. Pfeiffer, and P. Wambacq, "White paper on RF enabling 6G – opportunities and challenges from technology to spectrum," *6G Flagship Ecosystem*, Apr. 2021. [Online]. Available: https://www.6gchannel.com/items/6g-white-paper-rf-spectrum/

[4] C. Han, Y. Wang, Y. Li, Y. Chen, N. A. Abbasi, T. Kürner, and A. F. Molisch, "Terahertz wireless channels: A holistic survey on measurement, modeling, and analysis," *IEEE Communications Surveys & Tutorials*, vol. 24, no. 3, pp. 1670–1707, 2022.

[5] T. S. Rappaport, Y. Xing, O. Kanhere, S. Ju, A. Madanayake, S. Mandal, A. Alkhateeb, and G. C. Trichopoulos, "Wireless communications and applications above 100 GHz: Opportunities and challenges for 6G and beyond," *IEEE Access*, vol. 7, pp. 78 729–78 757, 2019.

[6] P. Tang, J. Zhang, H. Tian, Z. Chang, J. Men, Y. Zhang, L. Tian, L. Xia, Q. Wang, and J. He, "Channel measurement and path loss modeling from 220 GHz to 330 GHz for 6g wireless communications," *China Communications*, vol. 18, no. 5, pp. 19–32, 2021.

[7] J. Zhang, P. Tang, L. Yu, T. Jiang, and L. Tian, "Channel measurements and models for 6G: current status and future outlook," *Frontiers of information technology & electronic engineering*, vol. 21, no. 1, pp. 39–61, 2020.

[8] T. Kürner and S. Priebe, "Towards THz communications - status in research, standardization and regulation," *Journal of infrared, millimeter and terahertz waves*, vol. 35, no. 1, pp. 53–62, 2014.

[9] T. Schneider, A. Wiatrek, S. Preussler, M. Grigat, and R. Braun, "Link budget analysis for terahertz fixed wireless links," *IEEE Transactions on Terahertz Science and Technology*, vol. 2, no. 2, pp. 250–256, 2012.

[10] S. L. H. Nguyen, J. Järveläinen, A. Karttunen, K. Haneda, and J. Putkonen, "Comparing radio propagation channels between 28 and 140 GHz bands in a shopping mall," in *12th European Conference on Antennas and Propagation (EuCAP 2018)*, 2018, pp. 1–5.

[11] N. A. Abbasi, A. Hariharan, A. M. Nair, A. S. Almaiman, F. B. Rottenberg, A. E. Willner, and A. F. Molisch, "Double directional channel measurements for THz communications in an urban environment," in *ICC 2020 - 2020 IEEE International Conference on Communications (ICC)*, 2020, pp. 1–6.

[12] Y. Xing and T. S. Rappaport, "Propagation measurements and path loss models for sub-THz in urban microcells," in *ICC 2021 - IEEE International Conference on Communications*, 2021, pp. 1–6.

[13] Z. Chang, J. Zhang, P. Tang, L. Tian, Y. Yang, J. Lin, , and G. Liu, "3GPP-like THz channel modeling for indoor office and urban microcellular scenarios," *arXiv:2305.14997*, 2023.

[14] Y. Li, Y. Wang, Y. Chen, Z. Yu, and C. Han, "300 ghz channel measurement and characterization in the atrium of a building," in *2023 17th European Conference on Antennas and Propagation (EuCAP)*, 2023, pp. 1–5.

[15] Y. Lyu, Z. Yuan, M. Li, A. Mbugua, P. Kyösti, and W. Fan, "Enabling long-range large-scale channel sounding at sub-thz bands: Virtual array and radio-over-fiber concepts," *IEEE Communications Magazine*, Nov. 2022.

[16] B. Lee, A. Nix, and J. McGeehan, "A spatio-temporal ray launching propagation model for UMTS pico and microcellular environments," in *IEEE VTS 53rd Vehicular Technology Conference, Spring 2001. Proceedings (Cat. No.01CH37202)*, vol. 1, 2001, pp. 367–371 vol.1.

[17] S. Seidel and T. Rappaport, "A ray tracing technique to predict path loss and delay spread inside buildings," in *[Conference Record] GLOBECOM '92 - Communications for Global Users: IEEE*, 1992, pp. 649–653 vol.2.

[18] V. Degli-Esposti, F. Fuschini, E. M. Vitucci, and G. Falciasecca, "Speed-up techniques for ray tracing field prediction models," *IEEE Transactions on Antennas and Propagation*, vol. 57, no. 5, pp. 1469–1480, 2009.

[19] Y. Chen, Y. Li, C. Han, Z. Yu, and G. Wang, "Channel measurement and ray-tracing-statistical hybrid modeling for low-terahertz indoor communications," *IEEE Transactions on Wireless Communications*, vol. 20, no. 12, pp. 8163–8176, 2021.

[20] D. Dupleich, R. Müller, S. Skoblikov, M. Landmann, G. D. Galdo, and R. Thomä, "Characterization of the propagation channel in conference room scenario at 190 GHz," in *2020 14th European Conference on Antennas and Propagation (EuCAP)*, 2020, pp. 1–5.

[21] K. Guan, B. Peng, D. He, J. M. Eckhardt, H. Yi, S. Rey, B. Ai, Z. Zhong, and T. Kürner, "Channel sounding and ray tracing for intrawagon scenario at mmwave and sub-mmwave bands," *IEEE Trans. Antennas Propag.*, vol. 69, no. 2, pp. 1007–1019, 2021.

[22] Y. Li, Y. Chen, D. Yan, K. Guan, and C. Han, "Channel characterization and ray-tracing assisted stochastic modeling for urban vehicle-to-infrastructure terahertz communications," *IEEE Transactions on Vehicular Technology*, vol. 72, no. 3, pp. 2748–2763, 2023.

[23] S. Priebe and T. Kurner, "Stochastic modeling of THz indoor radio channels," *IEEE Transactions on Wireless Communications*, vol. 12, no. 9, pp. 4445–4455, 2013.

[24] C. Jansen, R. Piesiewicz, D. Mittleman, T. Kürner, and M. Koch, "The impact of reflections from stratified building materials on the wave propagation in future indoor terahertz communication systems," *IEEE Transactions on Antennas and Propagation*, vol. 56, no. 5, pp. 1413–1419, 2008.

[25] Y. Lyu, Z. Yuan, H. Gao, Q. Zhu, X. Zhang, and W. Fan, "Measurement-based channel characterization in a large hall scenario at 300 GHz," *China Communications*, vol. 20, no. 4, pp. 118–131, 2023.

[26] E. M. Vitucci, M. Zoli, F. Fuschini, M. Barbiroli, V. Degli-Esposti, K. Guan, B. Peng, and T. Kuerner, "Tri-band mm-wave directional channel measurements in indoor environment," in *2018 IEEE 29th Annual International Symposium on Personal, Indoor and Mobile Radio Communications (PIMRC)*, 2018, pp. 205–209.

[27] Remcom, "Wireless insite." [Online]. Available: https://www.remcom.com/wireless-insite

[28] ITU, "Recommendation P.2040." [Online]. Available: https://www.itu.int/rec/R-REC-P.2040/en

[29] Z. Yuan, J. Zhang, Y. Ji, G. F. Pedersen, and W. Fan, "Spatial non-stationary near-field channel modeling and validation for massive mimo systems," *IEEE Transactions on Antennas and Propagation*, vol. 71, no. 1, pp. 921–933, 2023.